Pharmacogn. Mag.
A multifaceted peer reviewed journal in the field of Pharmacognosy and Natural Products
www.phcog.com | www.phcog.net

ORIGINAL ARTICLE

Clinacanthus nutans Induced Reactive Oxygen Species-dependent Apoptosis and Autophagy in HCT116 Human Colorectal Cancer Cells

Kar Suen Wang, Chim Kei Chan, Ahmad Fadhlurrahman Ahmad Hidayat, Yau Hsiung Wong[1], Habsah Abdul Kadir

Institute of Biological Science, Faculty of Science, Institute of Biological Sciences, University of Malaya, Kuala Lumpur, [1]Department of Mathematics and Computer Science, School of Liberal Art and Sciences, Taylor's University Lakeside Campus, Subang Jaya, Selangor Darul Ehsan, Malaysia

Submitted: 08-07-2017 Revised: 16-08-2017 Published: 23-01-2019

ABSTRACT

Background: *Clinacanthus nutans* (Burm.f.) Lindau is a medicinal herb that is conventionally used for the treatment of skin rashes, insect bites, snake bites, diabetes, and cancer. **Objective:** Our study aims to investigate the apoptosis- and autophagy-inducing effects of *C. nutans* in HCT116 human colorectal cancer cells. **Materials and Methods:** Cytotoxicity of ethanol extract, hexane, ethyl acetate, and aqueous fractions of *C. nutans* against various cancer cell lines was determined via MTT assay. Apoptosis assays including annexin V, mito-ID, and Hoechst 33342/propidium iodide staining were carried out. The level of intracellular reactive oxidative species was determined using flow cytometry. Western blot analysis was carried out to assess the protein expression in *C. nutans* ethyl acetate fraction (CNEAF)-treated HCT116 cells. **Results:** CNEAF was found to exert the strongest cytotoxic effect against HCT116 cells (IC_{50} = 48.81 ± 1.44 μg/mL). CNEAF-induced apoptosis was evidenced by nuclear morphological alterations, phosphatidylserine externalization, dissipation of mitochondrial membrane potential, and elevation of intracellular reactive oxygen species (ROS) level. Dissipation of mitochondrial membrane potential was attributed to the upregulation of Bax and Bak accompanied by downregulation of Bcl-2 and Bcl-xL, leading to caspase-3, -9, -8, and -10 activation. Interestingly, an upregulation of death receptor 5 was detected, suggesting involvement of intrinsic and extrinsic pathways. In addition, the occurrence of autophagy by CNEAF was supported by LC-3 accumulation and p62 degradation. The reduction of intracellular ROS level by N-acetylcysteine showed that the apoptosis and autophagy induced by CNEAF is ROS dependent. **Conclusions:** CNEAF induced ROS-dependent apoptosis and autophagy on HCT116 cells.

Key words: Apoptosis, autophagy, *Clinacanthus nutans*, colorectal cancer, reactive oxygen species

SUMMARY

- Our findings have shown that CNEAF induced ROS-dependent apoptosis and autophagy mechanisms in HCT-116 human colorectal cancer cells.

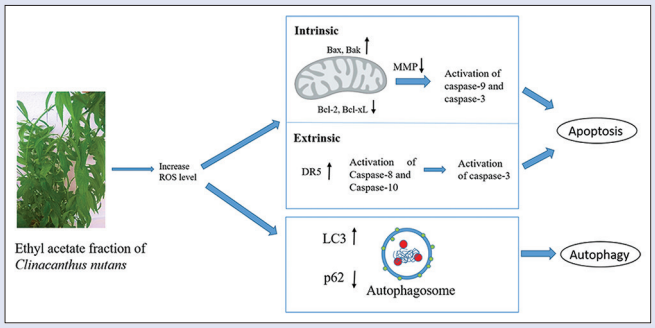

Abbreviations used: CNEAF: *Clinacanthus nutans* ethyl acetate fraction; ROS: Reactive oxygen species; PS: Phosphatidylserine; NAC:N-Acetyl Cysteine; Bax: Bcl-2-associated X; Bcl-2: B-cell lymphoma 2; DR-5: Death receptor 5 Bak: Bcl-2-antagonist/killer 1; Bcl-xL: B-cell lymphoma-extra large.

Correspondence:

Prof. Habsah Abdul Kadir,
Faculty of Science, Institute of Biological Sciences, University of Malaya, 50603 Kuala Lumpur, Malaysia. E-mail: habsah@um.edu.my

DOI: 10.4103/pm.pm_299_17

Access this article online
Website: www.phcog.com
Quick Response Code:

INTRODUCTION

Cancer is a destructive disease with a rise in the number of cases over the decades. Despite the huge efforts made by scientific community, there are no real breakthroughs in the advancement of drugs used during the last decade. Colorectal cancer has been identified as the third most common cancer worldwide and remains a major cause of mortality.[1] Therefore, more effective drugs and treatments are desperately needed. Toxicity, resistance, and limited effectiveness remain as big problems in existing cancer drugs.[2] Thus, traditional herbs can be used as an alternative route for cancer treatment or possibly a more effective way than cancer drugs.

Apoptosis, known as Type I programmed cell death, is described by alteration of nuclear morphology including cell shrinkage, condensation of both cytoplasm and nucleus, membrane blebbing, fragmentation of DNA, and apoptotic bodies formation.[3] Apoptosis signaling pathways are categorized into extrinsic and intrinsic pathways, which is executed by death receptors and various mitochondrial stimuli, respectively. The intrinsic pathway tightly governs by Bcl-2 family proteins that permeabilize the outer membrane of mitochondria. The ratio of pro-apoptotic and anti-apoptotic Bcl-2 family proteins is regarded as an apoptotic determinant. Activation of pro-apoptotic Bcl-2 family proteins shifted in favor of apoptosis, causing perturbation of mitochondrial membrane potential, resulted in opening of

Cite this article as: Wang KS, Chan CK, Ahmad Hidayat AF, Wong YH, Kadir HA. *Clinacanthus nutans* induced reactive oxygen species-dependent apoptosis and autophagy in HCT116 human colorectal cancer cells. Phcog Mag 2019;15:87-97.

mitochondrial membrane transition pore followed by the release of cytochrome c.[4] Subsequently, cytochrome c recruits apoptosome which further activates the caspase-9/-3 signaling cascades and lead to apoptosis induction. The extrinsic apoptosis pathway is initiated by the interaction of specific ligands and their respective death receptors. The receptors further recruit adaptor proteins and caspase-10/-8 to facilitate the formation of death-inducing signaling complex that transduces a downstream-signaling cascade.[5] Activation of caspase-8 can either directly trigger downstream executioner caspase-3 or through mitochondrial-mediated pathway by activating Bid to tBid.[6]

Autophagy is Type II programmed cell death, described as the sequestration of cellular material within autophagosomes and eventually degraded by lysosome. This process plays a vital role in homeostasis, cell differentiation, and development.[7,8] Normally, autophagy operates at the basal level in most cells to ensure that homeostasis functions properly. However, it will be increased rapidly when the cells undergo nutrient starvation, hypoxia, and getting rid of damaged cytoplasmic components and undergo architectural remodeling.[9] Ubiquitin-protein conjugating system is part of autophagy process, involved in the formation of autophagosomes. In LC3 conjugation system, LC3-I undergoes phosphatidylethanolamine conjugation by Atg7 and Atg3 to produce LC3-II. LC3-II is recruited to the membrane of phagophore to develop autophagosomes.[10,11] In addition, the p62 protein which complexes with LC3-II drives the ubiquitinated-protein aggregates into autophagosomes to facilitate the degradation.[12]

Clinacanthus nutans (Burm.f.) Lindau, also commonly known as Sabah snake grass, is an herb that belongs to the family of *Acanthaceae*. *C. nutans* is commonly distributed in tropical Asian countries such as Thailand, Malaysia, and Indonesia. The leaves of the plant are conventionally used as medicine and consumed in Southeast Asian countries for various purposes.[13] It has been conventionally used as an herbal medicine for allergic responses, snake bites, insect bites, herpes treatment, inflammation, and cancer.[14-18] The method of consuming *C. nutans* includes eating raw as vegetable, boiled and served as herbal tea, or mixed with juices and green tea.[17,19] Scientifically, multiple lines of evidence showed that extracts of *C. nutans* possessed cytotoxic and anticancer effects on various cancer cell lines, including human ovary cancer cell line (HeLa), human erythroleukemia cell line (K-562), human Burkitt's lymphoma cell line (Raji), and D24 melanoma cells.[20-22] We are the first to report the apoptosis- and autophagy-inducing effects of *C. nutans* ethyl acetate fraction (CNEAF) on HCT116 colorectal cancer cells.

MATERIALS AND METHODS

Cell culture

The selected cell lines were used in this study: human colorectal carcinoma cell line (HCT116), human colorectal adenocarcinoma cell line (HT-29), human cervix epidermoid carcinoma cell line (Ca Ski), human lung adenocarcinoma cell line (NCL-H23), human liver hepatocellular carcinoma cell line (Hep G2), human breast carcinoma (MCF-7), and human normal colon cell line (CCD-18Co). All the cell lines were purchased from the American Type Culture Collection (ATCC, Manassas, VA, USA). All cells were cultured in RPMI-1640 medium except Hep G2 that was cultured in Dulbecco's modified Eagle's medium (DMEM). The media were supplemented with (v/v) 10% fetal bovine serum (PAA Lab, Pasching, Austria) and 10 mL 100X antibiotic-antimycotic (Thermo Fisher Scientific, Waltham, Massachusetts, USA). The media were sterile-filtered and stored at low temperature. Hep G2 cell was cultivated in DMEM (Sigma, St. Louis, Missouri, USA) with the same amount of fetal bovine serum and antibiotic-antimycotic as RPMI-1640 medium. The cells were maintained in an incubator with 5% CO_2 and 37°C. The cells were checked regularly and subcultured to prevent any contamination. Trypan blue exclusion assay was done using a hemocytometer to perform viable cell count.

Clinacanthus nutans extract and fractions preparation

The plant *C. nutans* voucher specimen (No. KLU48654) deposited at the herbarium in the Institute of Biological Sciences, University of Malaya, Kuala Lumpur, Malaysia, was purchased from a local supplier. *C. nutans* dried leaves (1.5 kg) were soaked with 70% ethanol for 3 days at 35°C. The extract acquired was separated from residues by filtration. A rotary evaporator (Buchi) was used to concentrate the extract. Hexane was added to the dry extract (43.9 g) to obtain hexane soluble fraction. For the hexane-insoluble fraction, 1:1 ethyl acetate and water were used for further partitioning of both fractions, respectively. The dry ethyl acetate fraction was obtained using a rotary evaporator. The aqueous fractions were acquired by lyophilization. The ethanol extract of *C. nutans* leaves (CNEE), CNEAF, hexane fraction (CNHF), and aqueous fraction (CNAF) were dissolved in <0.5% v/v dimethyl sulfoxide (DMSO) before each assay.

In vitro cell proliferation assay

Viable cells were seeded and incubated for 24 h, followed by treatment of a range of concentrations (3.125–200 μg/mL) of *C. nutans* extract and fractions for 72 h. Vehicle DMSO was added to untreated cells instead of *C. nutans*. Next, MTT (5 mg/mL) was added into every well and incubated at room temperature without exposure to light for 4 h. After incubation, culture medium was completely removed and 150 μL of DMSO was added. The absorbance values were measured using a microplate reader (Asys UVM340, Biochrom, Cambourne, Cambridge, UK) at 570 nm and 650 nm as reference after 5 min of incubation.

Observation of nuclear morphology alteration by Hoechst 33342/propidium iodide

HCT116 cells (1×10^6 cells) were seeded in culture dish overnight and treated with CNEAF (50–200 μg/mL). DMSO was added into the negative control instead of CNEAF. Next, the cells were harvested and washed before Hoechst 33342 and propidium iodide (PI) dye staining in the dark for 30 min. The cells were viewed and quantified using a Leica DM1600B inverted fluorescence microscope and the fluorescence images were captured.

Annexin V/propidium iodide staining

Cells (1×10^6 cells) were plated and incubated for 24 h, followed by treatment with CNEAF (50–200 μg/mL) for 24 h. After treatment, 1X Annexin V-binding buffer was added to the cells after harvesting and washing. Cells were stained with PI dye and annexin V-fluorescein-isothiocyanate (FITC) before 15 min incubation without light exposure. The analysis of the cells was performed using quadrant statistics method using flow cytometry.

Assessment of mitochondrial membrane potential

Mito-ID® MP Detection Reagent (ENZO) (Lausen, Switzerland), a cationic carbocyanine dye, was used in this study to assess the alteration in matrix metalloproteinase (MMP). HCT116 cells (1×10^6 cells) were plated and incubated. The cells were then treated with varying concentrations (50–200 μg/mL) of CNEAF. Mitochondrial membrane potential was detected using Mito-ID® MP Detection Reagent for 15 min. Positive control was the carbonyl cyanide m-chlorophenyl hydrazone. Cells were then washed with phosphate-buffered saline and fluorescence signals were identified using FL1-A and FL2-A channels in flow cytometry.

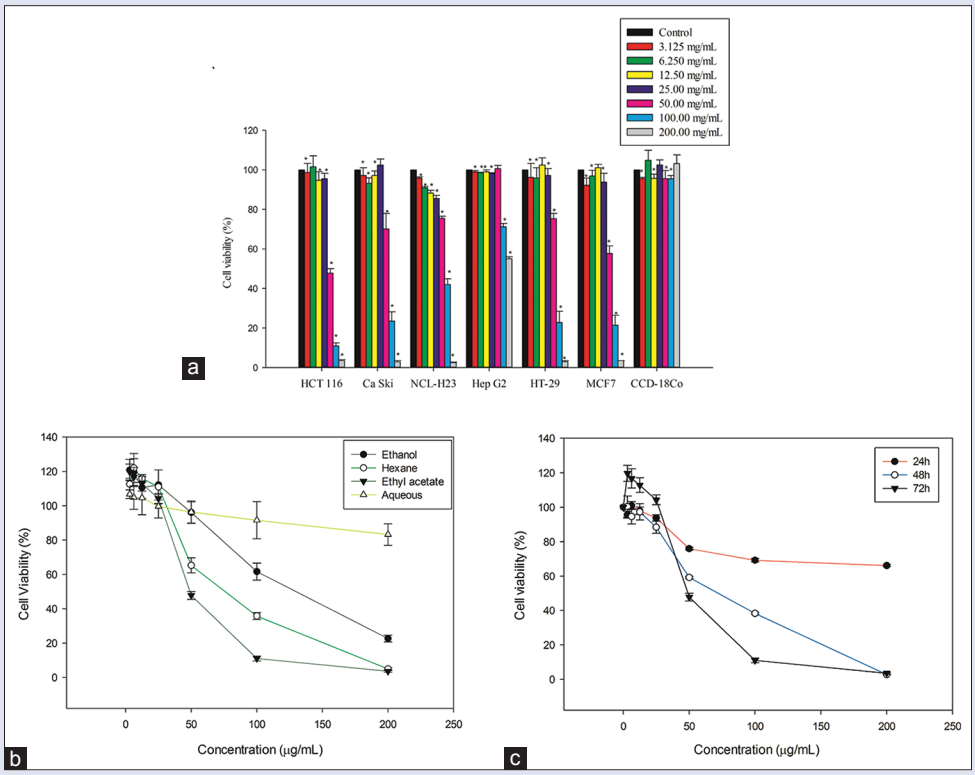

Figure 1: Cytotoxic effect of *Clinacanthus nutans* extract and fractions against various cancer cell lines. (a) Bar chart shows the cell viability percentage of cell lines when treated with different concentrations of *Clinacanthus nutans* ethyl acetate fraction for 72 h. (b) Line graph represents the cytotoxicity of ethanol extract of *Clinacanthus nutans*, *Clinacanthus nutans* hexane fraction, *Clinacanthus nutans* ethyl acetate fraction, and *Clinacanthus nutans* aqueous fraction against HCT116 cell line. (c) Line graph demonstrates the time-dependent cell viability of *Clinacanthus nutans* ethyl acetate fraction-treated HCT116. The data are represented as mean ± standard error of three independent experiments ($n = 9$). *$P < 0.05$

Acridine orange staining for autophagy

Plated cells were administrated with different concentrations (50–200 µg/mL) of CNEAF and incubated for 24 h. Acridine orange (1 µg/mL) was used to stain the harvested and washed cells for 15 min. On staining, 50 µL of 10% RPMI medium was supplemented to the cell suspension. The cell morphology was viewed under inverted fluorescence microscope and the fluorescence images were captured.

Determination of intracellular reactive oxygen species

For reactive oxygen species (ROS) determination, the fluorescence probe 2'-7'-dichlorofluorescein diacetate (DCFH-DA) was used. HCT116 cells were seeded and treated with CNEAF. NAC, a ROS inhibitor, was used as pretreatment. Tert-butyl hydroperoxide as a positive control while DMSO as negative control was used. After rested for 4 h, the cells were further washed and incubated for 1 h with addition of 40 µM of DCFH-DA. Next, the cells were harvested and subject to the determination of fluorescence intensity using flow cytometry.

Western blot analysis

Varying concentrations of CNEAF (50–200 µg/mL) were administrated to HCT116 cells and incubated for 24 h for cell lysate preparation. After 24 h treatment, the cells were harvested using RIPA buffer containing phosphatase and protease inhibitor. The cell lysate was centrifuged at 14,000 g for 25 min at 4°C. Without disrupting the pallet, the supernatant was collected and stored at −20°C and used for further analysis. Sodium dodecyl sulfate-polyacrylamide gel electrophoresis gel (10%–15%) was prepared according to the protocol. Total protein from each lysate was boiled at 95°C, loaded into the well of the gel, and run through electrophoresis. Next, the proteins were blotted onto a nitrocellulose membrane and blocked in skim milk or BSA for 1 h. Appropriate primary antibodies were added to the membrane and incubated at 4°C overnight. After incubation, the membrane was washed and incubated with its corresponding secondary antibody for 1 h. The washing and incubating processes were done on a shaker to increase binding efficiency. After another washing process, enhanced chemiluminescence detection kit (Bio-Rad, USA) was used for detection and gel documentation system was used for visualization. Protein content and concentrations were analyzed quantitatively and qualitatively using Vilber Lourmat software (Vilber Lourmat, Collégien, France).

Gas chromatography-mass spectrometry analysis of *Clinacanthus nutans* ethyl acetate fraction

The extract sample of *C. nutans* was performed using gas chromatography (GC), equipped with mass spectrometer (MS) single quadruple (GCMS-QP 2010 Plus). The detector was mass spectrometer and the column was DB-5MS, with length 30 m, diameter 0.25 mm, and 0.25 µm film. The concentration of sample was 20 ppm in 1 mL ethyl acetate. The carrier gas was helium, at a flow rate of 1 mL/min. The initial column temperature was set at 50°C and held for 4 min. Then, it was increased to 320°C at the ramp rate of 5°C/min and held for 10 min. The injector temperature was set at 280°C, and 1.0 µL of the diluted sample was injected manually in split mode. The scanning mode was obtained from the range m/z 40–700 and the electron ionization at 70 eV. The chromatograms of the sample were identified by comparing their mass spectra with NIST08 library data.

Statistical analysis

Each experiment was conducted in triplicate. The data from all the experiments were presented as means ± standard error of the mean. The statistical comparisons between respective control and treatments were calculated using one-way ANOVA, $P < 0.05$ which was considered to be statistically significant.

RESULTS

Cytotoxicity of *Clinacanthus nutans* extract and fractions on different cancer cell lines

Ca Ski, NCL-H23, HT-29, HCT116, MCF-7, Hep G2 cancer cells and CCD-18Co were treated to determine the cytotoxic effects of *C. nutans* extract and fractions using MTT assay. Different concentrations of CNEE, CNHF, CNEAF, and CNAF ranging from 3.125 to 400 µg/mL were used in treatment. All the IC_{50} values are calculated and summarized in Table 1. Figure 1 shows that CNEAF exhibited greater growth inhibitory effect on all the cancer cell lines when compared to others. Among the treated cell lines, CNEAF showed the most potent cytotoxic effect on human colon cancer HCT116 cells with the lowest IC_{50} value of 48.81 ± 1.44 µg/mL. In addition, CCD-18Co, a human normal colon cell, used as a representative of normal cells showed IC_{50} value of greater than 200 µg/mL. Thus, CNEAF was selected for further investigations on apoptosis induction in HCT116 cells.

Induction of nuclear morphological changes by *Clinacanthus nutans* ethyl acetate fraction

The staining of Hoechst 33342/PI was used to detect nuclear morphological changes in HCT116 cell in response to CNEAF treatment. Hoechst 33342 is a blue-fluorescence dye that stains the condensed chromatin in apoptotic cells while PI is a red-fluorescence dye that binds permanently to the DNA of dead cells. Thus, early apoptotic cells were stained with bright blue whereas late apoptotic cells displayed as bright blue and red, displaying a purple. Dead cells were presented in red. Figure 2 shows the morphological characteristics of apoptotic cells such as chromatin condensation, cell shrinkage, and DNA fragmentation increasing in appearance with the increasing concentrations of CNEAF.

Induction of early and late apoptosis by *Clinacanthus nutans* ethyl acetate fraction in HCT116 cells

Phosphatidylserine (PS) externalization is one of the distinctive features of apoptosis. During early apoptosis, externalization of PS results in

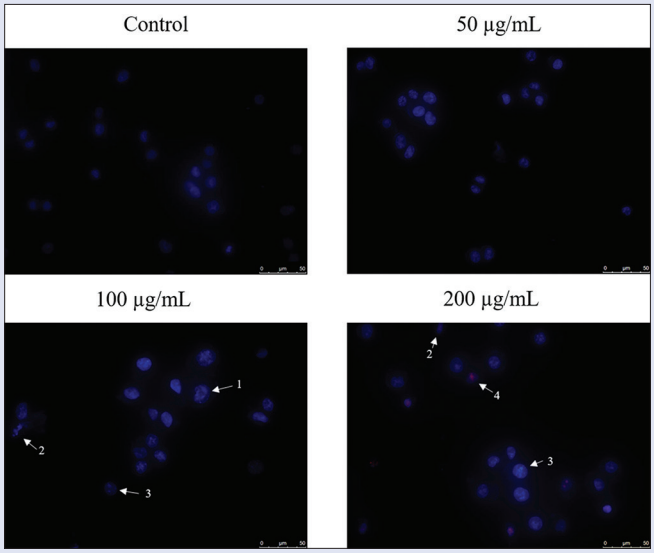

Figure 2: Nuclear morphological changes of HCT116 cells when treated with different concentrations of *Clinacanthus nutans* ethyl acetate fraction (×400). Arrows 1, 2, 3, and 4 indicate chromatin condensation, cell shrinkage, DNA fragmentation, and late apoptosis, respectively

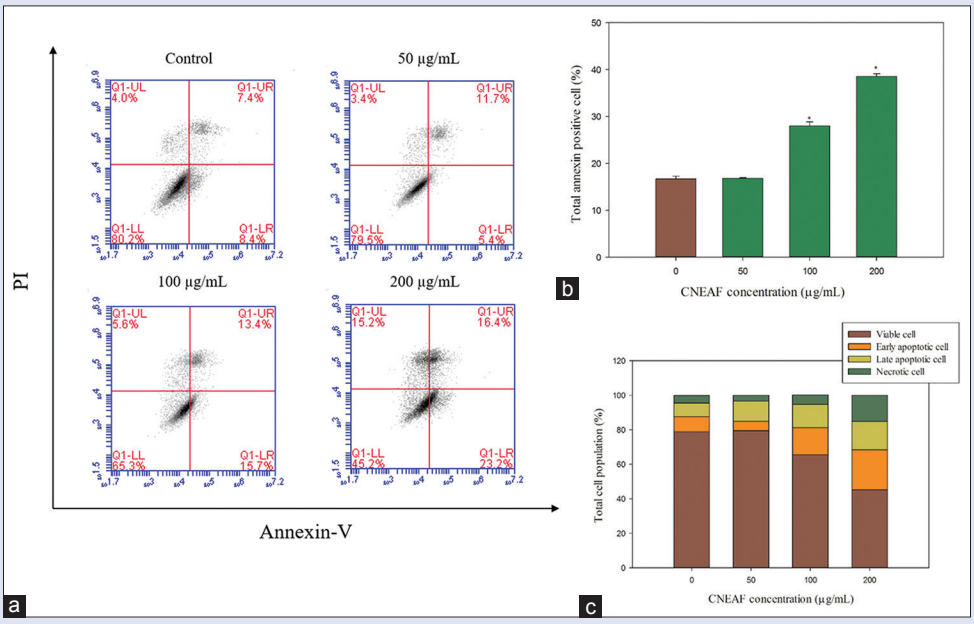

Figure 3: Induction of early and late apoptosis by *Clinacanthus nutans* ethyl acetate fraction (50, 100, and 200 µg/mL). (a) Bar chart displays the flow cytometry analysis of annexin V/propidium iodide staining. Lower left quadrant represents viable cells, lower right quadrant represents early apoptotic cells, upper left quadrant represents necrotic cells, and upper right quadrant represents late apoptotic cells. (b) Bar chart indicates the percentage of annexin V-positive cells. (c) Bar chart reveals the percentage of the cells in different stages. The data are expressed as mean ± standard error from three individual experiments. *$P < 0.05$

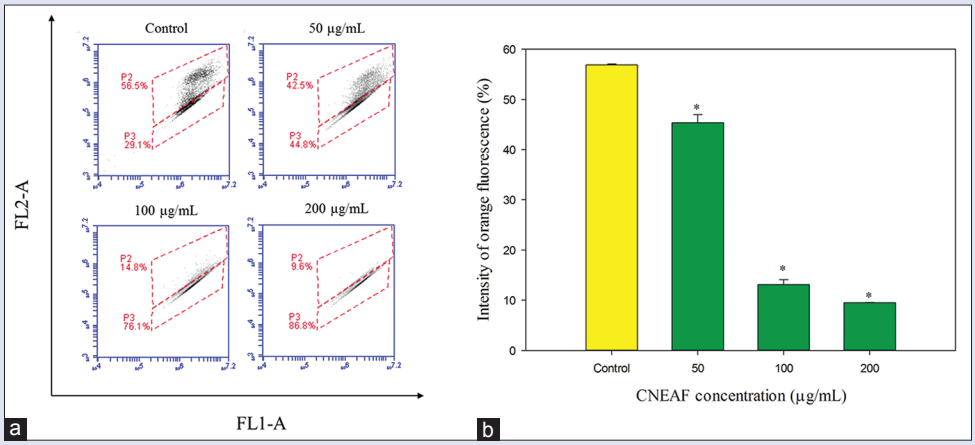

Figure 4: Dissipation of mitochondrial membrane potential in HCT116 cells induced by *Clinacanthus nutans* ethyl acetate fraction. (a) Flow cytometric fluorescence analysis of Mito-ID® membrane potential cytotoxicity assay on HCT116 cells. (b) Bar chart representing the percentage of orange fluorescence intensity on varying concentrations of *Clinacanthus nutans* ethyl acetate fraction. The data are expressed as mean ± standard error from three individual experiments. **P* < 0.05

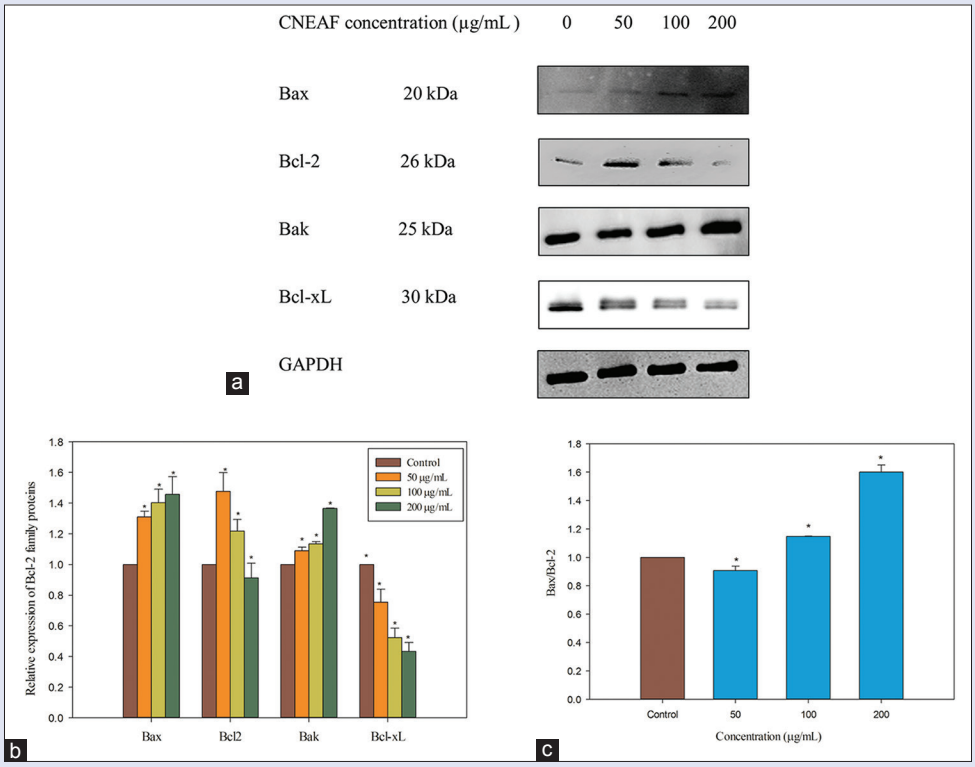

Figure 5: Effect of *Clinacanthus nutans* ethyl acetate fraction (50, 100, and 200 µg/mL) on Bcl-2 family protein expression in HCT116 cells. (a) Representative Western blot band intensity of Bak, Bax, Bcl-2, and Bcl-xL. (b) Bar chart shows the relative expression of Bcl-2, Bax, Bak and Bcl-xL. (c) Bar chart represents Bax to Bcl-2 ratio for different concentrations of *Clinacanthus nutans* ethyl acetate fraction. All the data are expressed as mean ± standard error from three independent experiments. **P* < 0.05

loss of membrane phospholipid asymmetry in the cells.[23] Annexin V is a phospholipid-protein that has a high affinity for PS while PI binds to DNA. Therefore, staining with FITC-annexin V and PI can be used to distinguish cells that undergo early and late apoptosis. The dual parametric dot plotted in Figure 3a displays the increase in the PS externalization when concentration of CNEAF increased. As shown in Figure 3b, the total number of annexin V-positive cells, which consisted of early and late apoptotic cells, was found elevated to 16.8 ± 0.15, 28 ± 0.86, and 38.6% ± 0.56% in a dose-dependent manner (50, 100, and 200 µg/mL).

Dissipation of mitochondrial membrane potential by *Clinacanthus nutans* ethyl acetate fraction in HCT116 cells

One of the early events of mitochondrial-mediated apoptosis is the loss of mitochondrial membrane potential. Changes in mitochondrial

membrane potential were detected by flow cytometer using Mito-ID® MP detection reagent, a fluorescent cationic carbocyanine dye that fluoresces either green or orange, depending on MMP status. In healthy cells, the dye fluoresces green in cytoplasm and orange in mitochondria. In an apoptotic cell, the dye exits mitochondria, showing a decreasing orange fluorescent fraction when run through the flow cytometer. In Figure 4a, HCT116 cells displayed increasing appearance of the green-fluorescent monomers in cytosol when concentrations of CNEAF increased. For the cells treated with the highest concentration of CNEAF, almost all the cells showed green-fluorescent monomers in the cytoplasm. As demonstrated in Figure 4b, the reduction of mitochondrial membrane potential was significant in HCT116 cells when treated with increasing concentrations of CNEAF. The intensity of the orange fluorescence decreased from control to 45.4% ± 1.60%, 13.1% ± 0.98%, and 9.5% ± 0.06% with respective concentrations of CNEAF 50, 100, and 200 µg/mL.

Modulation of Bcl-2 family member proteins expression by *Clinacanthus nutans* ethyl acetate fraction

Mitochondrial involvement in apoptosis is regulated by Bcl-2 family proteins that are divided into anti-apoptotic and pro-apoptotic proteins. To study the effect of CNEAF on apoptosis-related proteins, we examined the expression of four members of the Bcl-2 family proteins including Bax, Bak, Bcl-xL, and Bcl-2 proteins by Western blot analysis. Treatment with CNEAF in HCT116 cells resulted in upregulation of the pro-apoptotic Bax and Bak proteins, as well as downregulation of anti-apoptotic Bcl-2 and Bcl-xL proteins, in a dose-dependent manner [Figure 5]. CNEAF also elevated the ratio of Bax to Bcl-2 by 1.60-fold in HCT116 treated with 200 µg/mL of CNEAF. These data further suggested that CNEAF induced apoptosis via the mitochondrial intrinsic pathway in HCT116 cells.

Activation of extrinsic and intrinsic apoptosis in *Clinacanthus nutans* ethyl acetate fraction-treated cells

Caspases are essential in orchestrating the intrinsic and extrinsic apoptosis pathways. Here, the protein levels of apoptotic proteins including caspase-3, -9, -8, and -10, cleaved caspase-9, and DR5 were evaluated using Western blot analysis [Figure 6b]. CNEAF treatment caused the activation of caspase-9, -3, -8, and -10 which were observed in a dose-dependent manner. As shown in Figure 6a, the expression of caspase-3, -9, -8, and -10 proteins decreased to 0.44 ± 0.02, 0.49 ± 0.01, 0.52 ± 0.10, and 0.43 ± 0.06, respectively, when treated with 200 µg/mL of CNEAF. The expression of cleaved caspase-9 and DR5 was increased to 2.21 ± 0.05 and 2.18 ± 0.11, respectively, in CNEAF-treated

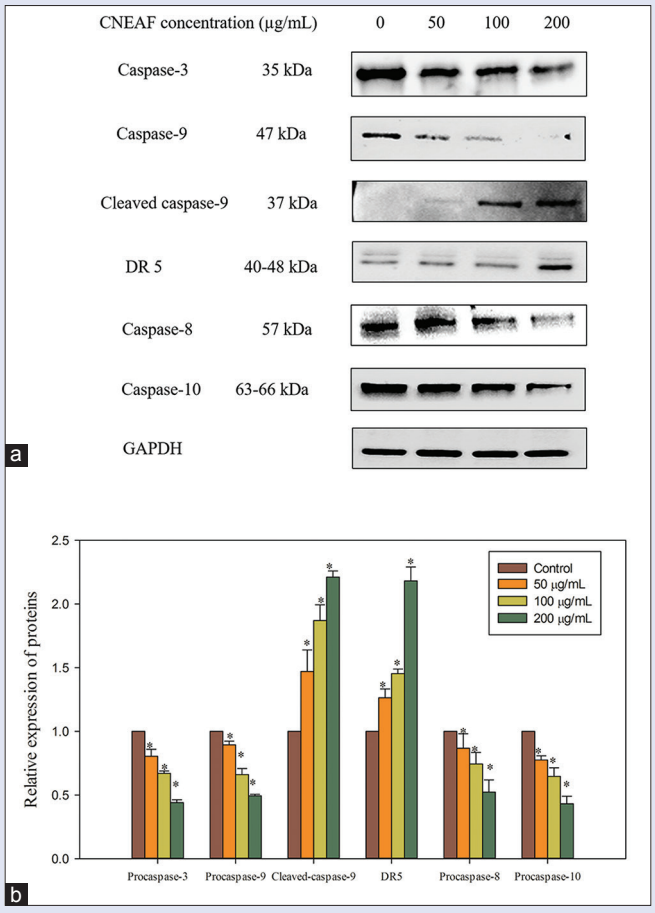

Figure 6: Activation of extrinsic and intrinsic apoptosis in *Clinacanthus nutans* ethyl acetate fraction-treated HCT116 cells. (a) Representative Western blot band intensity of apoptosis-related proteins. (b) Bar chart reveals the relative expression of caspases and DR5 proteins. All the data are expressed as mean ± standard error for three independent experiments. *$P < 0.05$

Table 1: IC_{50} values of the extract and fractions of *Clinacanthus nutans* in different types of cancer and normal cell lines

Cell lines	IC_{50} (µg/mL)			
	Ethanol extract	Hexane fraction	Ethyl acetate fraction	Aqueous fraction
HCT116	124.70±9.66	67.44±4.36	48.81±1.44	>200
HT-29	171.57±2.48	93.64±8.25	68.25±3.08	>200
Ca Ski	167.55±6.05	84.56±1.18	55.42±0.06	>200
NCL-H23	>200	123.02±3.33	87.03±4.26	>200
Hep G2	>200	>200	>200	>200
MCF-7	>200	84.77±3.43	57.75±4.00	>200
CCD-18Co	NA	NA	>200	NA

The data represent mean±standard error of three independent experiment (n=9)

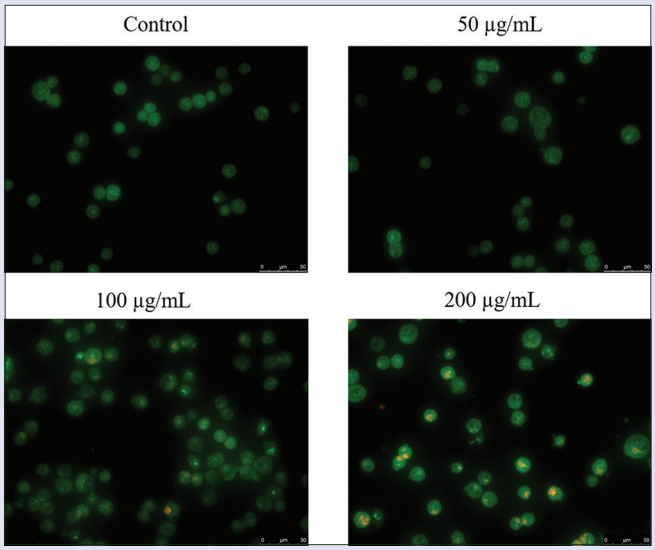

Figure 7: Formation of acidic vesicles organelles induced by different concentrations of *Clinacanthus nutans* ethyl acetate fraction (50, 100, and 200 µg/mL) in HCT116 cells. The cells were observed under fluorescence microscope (×400)

HCT116 cells (200 μg/mL). These results suggested the involvement of intrinsic and extrinsic pathways by CNEAF in HCT116 cells.

Induction of autophagy in *Clinacanthus nutans* ethyl acetate fraction-treated HCT116 cells

Formation of acidic vesicular organelles (AVOs) is one of the characteristics of autophagic cells.[24,25] Acridine orange stained the whole cells in green fluorescence except for the acidic compartments, which fluoresces red. The formation of acidic vacuoles in autophagosomes is an indication of autophagy; thus, the number of red fluorescence indicates the amount of autophagy in the cell. Figure 7 shows the increased formation of AVOs in CNEAF-treated HCT116 cells when compared to vehicle control.

Regulation of autophagy-related proteins in *Clinacanthus nutans* ethyl acetate fraction-treated HCT116 cells

Autophagy is another process that takes part in cell death and tumor prevention.[7,26] Microtubule-associated protein 1 light chain 3 (LC3) protein is one of the key autophagy-related proteins, which was evaluated in CNEAF-treated cells. Next, the regulation of p62 was investigated in HCT116 cells on exposure to 200 μg/mL of CNEAF. Ubiquitin-binding protein, p62, is an important marker for autophagy induction, and it is essential for the formation of inclusion body in autophagy. As shown in Figure 8a and b, CNEAF induced dose-dependent accumulation of LC3-II and degradation of p62 as compared to the control.

Effect of *Clinacanthus nutans* ethyl acetate fraction on reactive oxygen species level in HCT116 cells

The intracellular ROS level can be detected using DCFH-DA. The right shift in the histogram indicated an increase in the intracellular ROS level. In the current study, the intracellular ROS level was elevated dose dependently in HCT116 cells when treated with CNEAF [Figure 9]. The intracellular ROS levels were elevated by 2.20 ± 0.09, 2.41 ± 0.003, and 4.10 ± 0.01 folds when treated with 50, 100, and 200 μg/mL of CNEAF, respectively.

Reactive oxygen species-dependent apoptosis in HCT116 cells

N-acetyl cysteine (NAC) was used as an inhibitor to impair the production of ROS. The MTT results showed increase in cell viability in CNEAF-treated HCT116 cells in the presence of 1 mM NAC [Figure 10a]. The intracellular ROS level significantly reduced in HCT116 cells treated with 200 μg/mL of CNEAF in the presence of NAC when compared to the group without NAC [Figure 10b]. Western blot analysis in Figure 10c shows an inactivation of caspase-3 and -9 when CNEAF-treated HCT116 cells were pretreated with 1 mM NAC.

Reactive oxygen species-dependent autophagy in HCT116 cells

Acridine orange assay and Western blot analysis were repeated using 1 mM NAC to assess the ROS dependency of autophagy-inducing effect of CNEAF in HCT116 cells. According to the fluorescence images of acridine orange staining shown in Figure 11a, there was not much change when the control cells were pretreated with NAC. However, there was less red fluorescence displayed in CNEAF-treated HCT116 cells pretreated with 1 mM NAC compared with HCT116 cells without pretreatment. Figure 11b shows a decrease in LC3 protein expression when compared to CNEAF-treated HCT116 cells pretreated with NAC or without NAC.

Gas chromatography-mass spectrometry profiles of *Clinacanthus nutans* ethyl acetate fraction

The main constituents in the CNEAF were analyzed using GC-MS [Figure 12]. By comparing the mass spectra with NIST08 library data, the six components identified were diethyl phthalate, 9-eicosyne, hexadecanoic acid, stigmasterol, beta-sitosterol, and lupeol [Table 2].

DISCUSSION

The present study suggests that apoptosis and autophagy contribute to the anticancer activity of CNEAF through the generation of ROS. It was

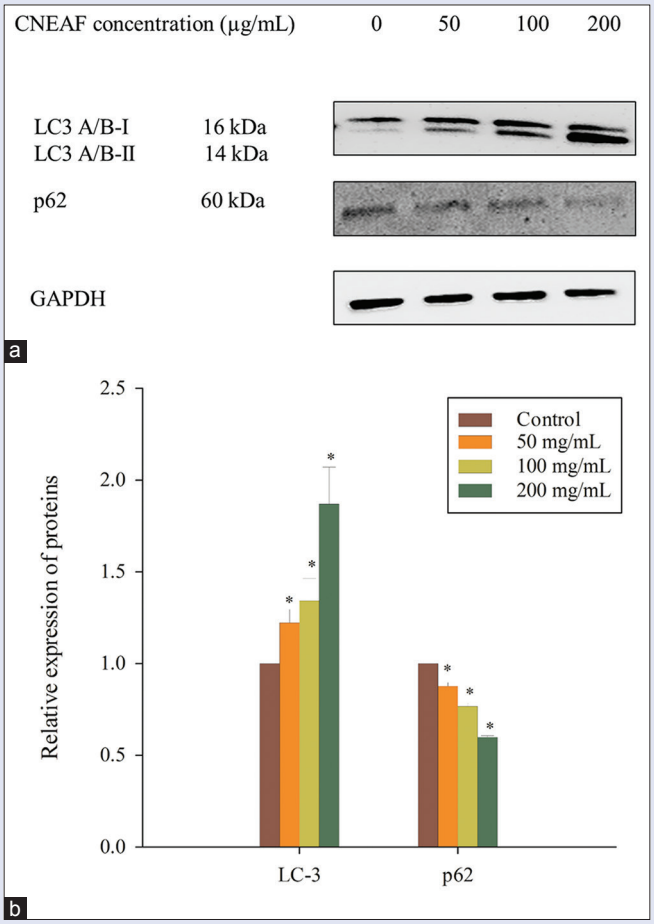

Figure 8: Autophagy-related protein, LC-3 and p62 protein expressions in HCT116 cells when treated with *Clinacanthus nutans* ethyl acetate fraction. (a) Western blot band intensity of LC-3 and p62. (b) Bar chart displays the relative expression of LC-3 and p62 proteins. All the data are expressed as mean ± standard error from three independent experiments. *$P < 0.05$

Table 2: Identified components in *Clinacanthus nutans* ethyl acetate fraction by gas chromatography-mass spectrometry

Compounds	M.W. (g/mol)	M.F.	Retention time (min)
Diethyl phthalate	222.2	$C_{12}H_{14}O_4$	27.806
9-Eicosyne	278.5	$C_{20}H_{38}$	33.279
Hexadecanoic acid	256.4	$C_{16}H_{32}O_2$	35.863
Stigmasterol	412.7	$C_{29}H_{48}O$	55.571
Beta-sitosterol	414.7	$C_{29}H_{50}O$	56.346
Lupeol	426.8	$C_{30}H_{50}O$	57.456

M.W.: Molecular weight; M.F.: Molecular formula

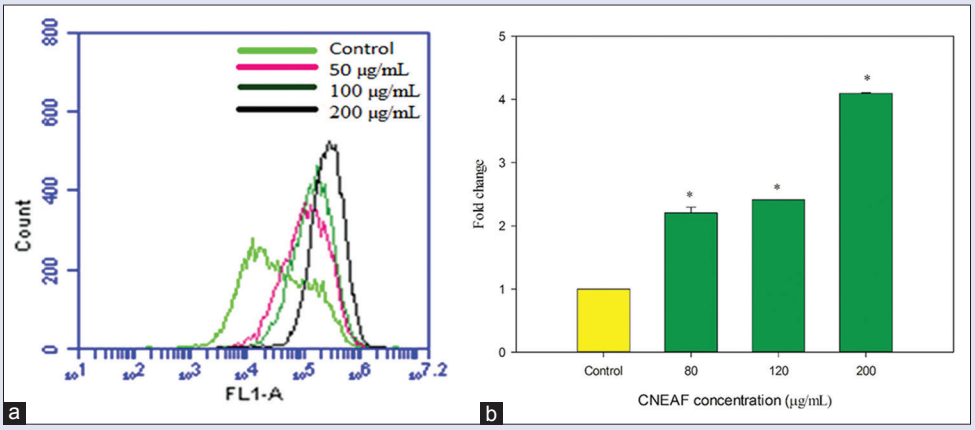

Figure 9: Intracellular reactive oxygen species induction in HCT116 cells treated with various concentration of *Clinacanthus nutans* ethyl acetate fraction (a) Histogram illustrates the intracellular reactive oxygen species level in HCT116 cells. (b) Bar chart represents the fold change of intracellular reactive oxygen species level in HCT116 cells. The data are represented as the mean ± standard error of three independent experiments. *$P < 0.05$

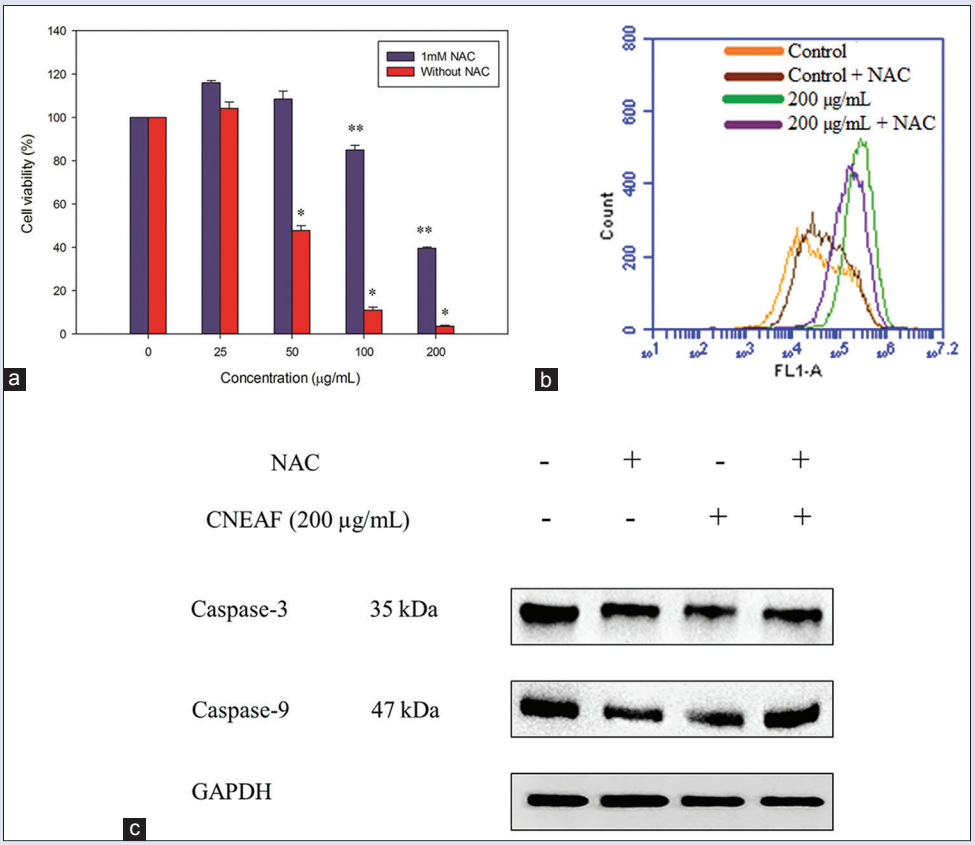

Figure 10: Involvement of oxidative stress stimuli, reactive oxygen species, and apoptosis induction by *Clinacanthus nutans* ethyl acetate fraction. (a) Bar chart displays the MTT assay of *Clinacanthus nutans* ethyl acetate fraction-treated HCT116 when pretreated in the presence and absence of 1 mM N-acetyl cysteine. (b) Histogram displays the intracellular reactive oxygen species level in the presence and absence of 1 mM N-acetyl cysteine for 1 h on untreated and treated HCT116 with 200 µg/mL of *Clinacanthus nutans* ethyl acetate fraction. (c) Western blot analysis of caspase-3 and caspase-9 proteins pretreated with 1 mM N-acetyl cysteine. The data are represented as the mean ± standard error of three independent experiments. Asterisks indicate significantly different value from control (*$P < 0.05$). Double asterisks indicate significantly different value compared to the treated cells without 1 mM N-acetyl cysteine

found that CNEAF induced apoptosis in HCT116 cells through intrinsic and extrinsic pathways. In addition to the induction of apoptosis, CNEAF also caused HCT116 cell cytotoxicity through the induction of autophagy. Furthermore, the interplay of oxidative stress and the cell death mechanism were studied in the present study. Our findings demonstrated that CNEAF could induce apoptosis and autophagy in HCT116 cells in response to the stimulation of ROS.

Apoptosis is implicated as a potential therapeutic strategy for the intervention of cancer as it plays important roles in cellular development, differentiation, homeostasis, and removal of defective cells.[26] In the present study, significant nuclear morphological changes, increase in annexin V-FITC-positive stained cells, and disruption of mitochondrial membrane potential were observed in HCT116 cells upon exposure to CNEAF, suggesting the association between

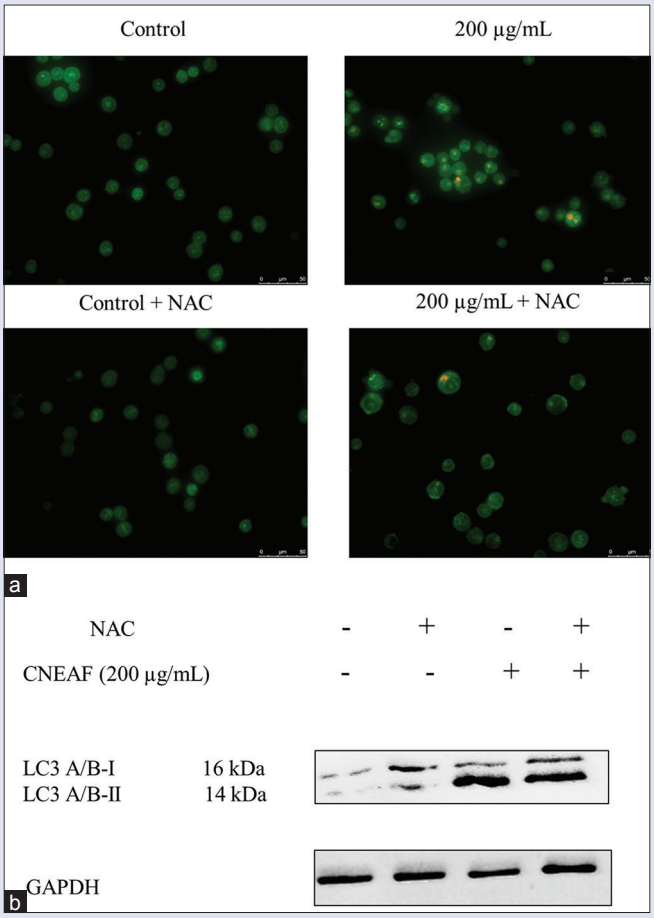

Figure 11: Involvement of oxidative stress stimuli, reactive oxygen species, and autophagy induction by *Clinacanthus nutans* ethyl acetate fraction (a) Fluorescence images indicate the acidic vesicular organelles formation in HCT116 cells which treated with 200 µg/mL *Clinacanthus nutans* ethyl acetate fraction in the presence or absence of 1 mM N-acetyl cysteine (×400). (b) Western blot analysis of LC3 protein in the presence of 1 mM N-acetyl cysteine

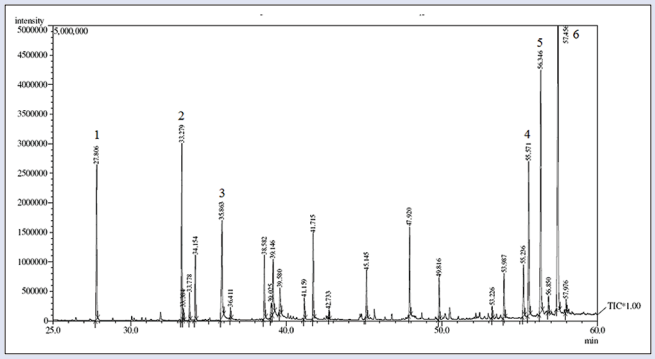

Figure 12: Gas chromatography-mass spectrometry analysis of *Clinacanthus nutans* ethyl acetate fraction

mitochondria and apoptosis-inducing effects of CNEAF. Depolarization of mitochondrial membrane potential is attributed to the dysregulation of Bcl-2 family members which are governed by pro-apoptotic proteins (e.g., Bak and Bax) and anti-apoptotic proteins (e.g., Bcl-2 and Bcl-xL).[27,28] In the present study, CNEAF treatment resulted in a downregulation of anti-apoptotic Bcl-2 and Bcl-xL proteins along with an upregulation of pro-apoptotic Bax and Bak proteins. These findings suggested that dissociation of anti-apoptotic Bcl-2 proteins enhanced the oligomerization of pro-apoptotic Bcl-2 proteins, leading to permeabilization of mitochondrial outer membrane and releasing a multitude of apoptotic substrates via a series of caspase cascade.[29] The intrinsic pathway, also known as mitochondrial-mediated apoptotic pathway, is governed by mitochondria via the sequential activation of initiator caspase-9 and the executioner caspase-3/-7. In consistent with this, our results demonstrated that the loss of mitochondrial membrane potential preceded the activation of caspase cascades involving caspase-9 and -3 by CNEAF in HCT116 cells. It is well documented that extrinsic pathway is initiated by the binding of ligands to their death receptors, including TNF-Rs and FasL.[5] Integration of intracellular signals further recruits the initiator caspase-8 and -10, which mediate apoptosis directly via effector caspases-3/-7 or indirectly through intrinsic pathway.[30] Accordingly, CNEAF was shown to induce extrinsic pathway by activating DR5 and sequentially activating caspase-8, -10, and-3. These collective findings strongly suggested that CNEAF mediated apoptosis through the extrinsic and intrinsic pathways in HCT116 cells.

Apart from apoptosis, an alternative which recently emerged and raises interest in cancer treatment is autophagy. Autophagy is orchestrated by lysosomal enzymes which digests and recycles the aged or dysfunction proteins and organelles.[7,8] The degradation of dysfunction components occurs on fusion between autophagosomes and lysosomes.[31] A panel of natural products has been identified to trigger cell death by initiating autophagy signaling transduction and is able to confer both apoptotic and autophagic cell death. Interestingly, it was found that CNEAF induced autophagy in HCT116 cells which is evidenced by an apparent increase of AVOs. In addition, LC3-II protein, one of the essential autophagy determinants, was found to significantly accumulate concomitantly with degradation of p62 protein in CNEAF-treated HCT116 cells. These collective data strongly suggested that CNEAF elicited pro-death autophagy in HCT116 cells.

Numerous lines of evidence have established that ROS are an essential signaling mediator in governing a diverse signal transduction pathways, particularly in inducing apoptosis and autophagy.[32-35] Aberrant generation of ROS in cancer cells renders the cells more susceptible to DNA damage, drug sensitivity, and cell death.[36] Our results suggested that an accumulation of ROS was mediated in HCT116 cells on exposure of CNEAF. On the contrary, the ROS scavenger, NAC, significantly impeded the intracellular ROS generation induced by CNEAF and concurrently restored the cell viability of HCT116. Notably, ROS participates in the initiation of apoptosis by triggering the mitochondrial membrane potential disruptions, resulting in the release of cytochrome c and caspases cascades activation.[37] In a previous report, carnisol was shown to induce apoptosis in response to oxidative stress in HCT116 cells and was reversed by NAC, as evidenced by reduced cleaved caspase-3, suggesting ROS-dependent activation of caspase-3.[38] In consistency with this, the presence of NAC abrogated the CNEAF-induced activation of caspase-3 and -9. Thus, these findings proposed that the onset of apoptosis triggered by CNEAF was preceded by the ROS-dependent caspase activation. It is noteworthy that the impairment of lysosomes in cancer cells might be a possible mechanism of the autophagic cell death following overproduction of ROS. Moreover, an acute generation of ROS can disrupt lysosomal membrane and lead to the leakage of hydrolytic enzymes which eventually caused autophagic cell death.[39-41] As recently reported, ginsenoside compound K from ginseng was found to induce ROS-dependent autophagy in HCT116 cells, and NAC reversed the level of LC3-II expression.[42] In the present study, apart from NAC activation of caspases, NAC limited the accumulation of LC3-II protein and the formation of AVO, which was induced by CNEAF. These collective

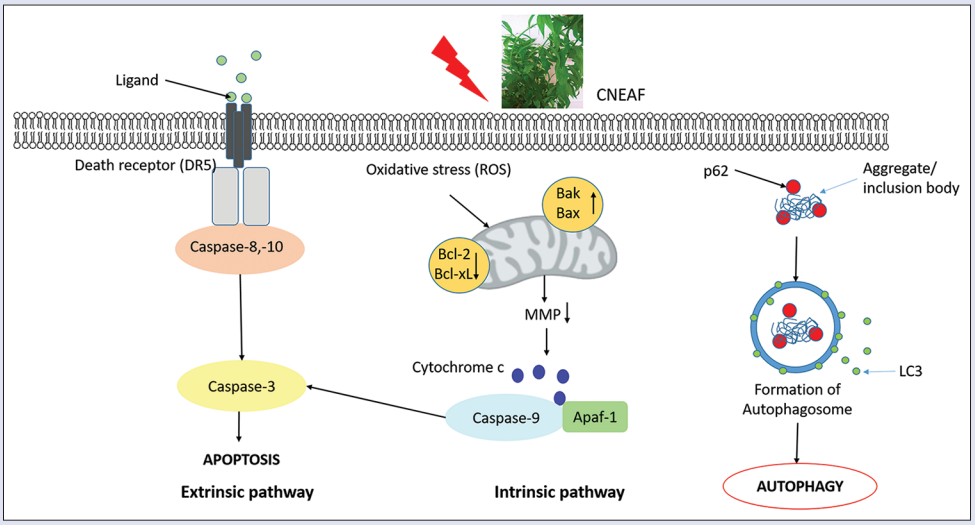

Figure 13: Graphical illustration of the apoptosis and autophagy cell death effects conferred by *Clinacanthus nutans* ethyl acetate fraction in HCT116 cells

findings demonstrated that on the withdrawal of ROS stimulation, both the CNEAF-induced apoptosis and autophagy were impeded indicating that the initiation of apoptotic and autophagic cell death was attributable to the ROS generation induced by CNEAF. Nevertheless, interplay of the apoptosis and autophagy induced by CNEAF warrants further investigations, which may provide further insight for the mechanisms of apoptosis and autophagy regulation as therapeutic strategy.

Apoptosis- and autophagy-inducing effects may be attributable to the presence of the phytochemical constituents in CNEAF. According to the phytochemical profiling by GC-MS analysis, several phytochemical constituents identified in CNEAF have shown apoptosis-inducing effects in various cancer cell lines. For instance, lupeol has been widely reported for its anticancer effect against various cancer cells such as oral cancer,[43] pancreatic cancer,[44] gallbladder cancer,[45] prostate cancer,[46] and colorectal cancer.[47] In addition, β-sitosterol was also shown to possess chemopreventive potential in the development of several types of cancer such as colon, prostate, and breast cancer.[48-50] Hence, the presence of these phytochemicals in CNEAF may synergistically responsible to the apoptosis-inducing effect which suggested from our results.

CONCLUSIONS

Briefly, our findings suggest that CNEAF induced ROS-dependent apoptosis and autophagy in HCT116 human colorectal cancer cells which is depicted in Figure 13. CNEAF functions as a ROS-inducing agent and mediates intrinsic apoptosis accompanied by the modulation of Bax/Bcl-2 ratio and activation of caspase-3 and -9. In addition, CNEAF initiates extrinsic pathway by recruiting death receptor DR5 and activating caspase-8 and -10, eventually leading to intrinsic apoptosis. Intriguingly, autophagy is conferred by CNEAF evidenced by the accumulation of AVO and LC3-II along with the degradation of p62 proteins. In conclusion, our present study suggested that *C. nutans* holds a therapeutic potential in the intervention of colorectal cancer. Isolation of bioactive phytochemicals from *C. nutans* may inspire the development of complementary alternative medicines to target human colorectal cancers.

Financial support and sponsorship

Nil.

Conflicts of interest

There are no conflicts of interest.

REFERENCES

1. Ferlay J, Soerjomataram I, Dikshit R, Eser S, Mathers C, Rebelo M, *et al.* Cancer incidence and mortality worldwide: Sources, methods and major patterns in GLOBOCAN 2012. Int J Cancer 2015;136:E359-86.
2. Temraz S, Mukherji D, Alameddine R, Shamseddine A. Methods of overcoming treatment resistance in colorectal cancer. Crit Rev Oncol Hematol 2014;89:217-30.
3. Edinger AL, Thompson CB. Death by design: Apoptosis, necrosis and autophagy. Curr Opin Cell Biol 2004;16:663-9.
4. Bold RJ, Termuhlen PM, McConkey DJ. Apoptosis, cancer and cancer therapy. Surg Oncol 1997;6:133-42.
5. Ashkenazi A. Targeting the extrinsic apoptosis pathway in cancer. Cytokine Growth Factor Rev 2008;19:325-31.
6. Wei MC, Lindsten T, Mootha VK, Weiler S, Gross A, Ashiya M, *et al.* TBID, a membrane-targeted death ligand, oligomerizes BAK to release cytochrome c. Genes Dev 2000;14:2060-71.
7. Klionsky DJ. Autophagy: From phenomenology to molecular understanding in less than a decade. Nat Rev Mol Cell Biol 2007;8:931-7.
8. Meijer AJ, Dubbelhuis PF. Amino acid signalling and the integration of metabolism. Biochem Biophys Res Commun 2004;313:397-403.
9. Levine B, Yuan J. Autophagy in cell death: An innocent convict? J Clin Invest 2005;115:2679-88.
10. Feng Y, He D, Yao Z, Klionsky DJ. The machinery of macroautophagy. Cell Res 2014;24:24-41.
11. Kabeya Y, Mizushima N, Yamamoto A, Oshitani-Okamoto S, Ohsumi Y, Yoshimori T, *et al.* LC3, GABARAP and GATE16 localize to autophagosomal membrane depending on form-II formation. J Cell Sci 2004;117:2805-12.
12. Bjørkøy G, Lamark T, Brech A, Outzen H, Perander M, Overvatn A, *et al.* P62/SQSTM1 forms protein aggregates degraded by autophagy and has a protective effect on huntingtin-induced cell death. J Cell Biol 2005;171:603-14.
13. Yahaya R, Dash GK, Abdullah MS, Mathews A. *Clinacanthus nutans* (Burm. F.) Lindau: An useful medicine plant of South-East Asia. Int J Pharmacogn Phytochem Res 2015;7:1244-50.
14. Alam A, Ferdosh S, Ghafoor K, Hakim A, Juraimi AS, Khatib A, *et al. Clinacanthus nutans*: A review of the medicinal uses, pharmacology and phytochemistry. Asian Pac J Trop Med 2016;9:402-9.
15. Pongmuangmul S, Phumiamorn S, Sanguansermsri P, Wongkattiya N, Fraser IH, Sanguansermsri D. Anti-herpes simplex virus activities of monogalactosyl diglyceride and digalactosyl diglyceride from *Clinacanthus nutans*, a traditional Thai herbal medicine. Asian Pac J Trop Biomed 2016;6:192-7.
16. Sakdarat S, Shuyprom A, Pientong C, Ekalaksananan T, Thongchai S. Bioactive constituents from the leaves of *Clinacanthus nutans* Lindau. Bioorg Med Chem 2009;17:1857-60.

17. Shim SY, Aziana I, Khoo BY. Perspective and insight on *Clinacanthus nutans* Lindau in traditional medicine. Int J Integr Biol 2103;14:7-9.
18. Tuntiwachwuttikul P, Pootaeng-On Y, Phansa P, Taylor WC. Cerebrosides and a monoacylmonogalactosylglycerol from *Clinacanthus nutans*. Chem Pharm Bull (Tokyo) 2004;52:27-32.
19. Aslam MS, Awan AJ, Uzair M, Farooq U. family *Acanthaceae* and genus *Aphelandra*: Ethnopharmacological and phytochemical review. Int J Pharm Pharm Sci 2014;6:44-55.
20. Arullappan S, Rajamanickam P, Thevar N, Kodimani CC. *In vitro* screening of cytotoxic, antimicrobial and antioxidant activities of *Clinacanthus nutans* (*Acanthaceae*) leaf extracts. Trop J PharmRes 2014;13:1455.
21. Fong SY, Piva T, Dekiwadia C, Urban S, Huynh T. Comparison of cytotoxicity between extracts of *Clinacanthus nutans* (Burm. F.) Lindau leaves from different locations and the induction of apoptosis by the crude methanol leaf extract in D24 human melanoma cells. BMC Complement Altern Med 2016;16:368.
22. Yong YK, Tan JJ, Teh SS, Mah SH, Ee GC, Chiong HS, *et al. Clinacanthus nutans* extracts are antioxidant with antiproliferative effect on cultured human cancer cell lines. Evid Based Complement Alternat Med 2013;2013:462751.
23. Koopman G, Reutelingsperger CP, Kuijten GA, Keehnen RM, Pals ST, van Oers MH, *et al.* Annexin V for flow cytometric detection of phosphatidylserine expression on B cells undergoing apoptosis. Blood 1994;84:1415-20.
24. Bursch W, Ellinger A, Gerner C, Fröhwein U, Schulte-Hermann R. Programmed cell death (PCD). Apoptosis, autophagic PCD, or others? Ann N Y Acad Sci 2000;926:1-2.
25. Paglin S, Hollister T, Delohery T, Hackett N, McMahill M, Sphicas E, *et al.* A novel response of cancer cells to radiation involves autophagy and formation of acidic vesicles. Cancer Res 2001;61:439-44.
26. Tan ML, Ooi JP, Ismail N, Moad AI, Muhammad TS. Programmed cell death pathways and current antitumor targets. Pharm Res 2009;26:1547-60.
27. Edlich F, Martinou JC. Bcl-2 Protein interplay on the outer mitochondrial membrane. In: Hockenbery DM, editor. Mitochondria and Cell Death. New York, NY: Springer New York; 2016. p. 69-83.
28. Tsujimoto Y. Role of bcl-2 family proteins in apoptosis: Apoptosomes or mitochondria? Genes Cells 1998;3:697-707.
29. Fan TJ, Han LH, Cong RS, Liang J. Caspase family proteases and apoptosis. Acta Biochim Biophys Sin (Shanghai) 2005;37:719-27.
30. Fulda S. Targeting extrinsic apoptosis in cancer: Challenges and opportunities. Semin Cell Dev Biol 2015;39:20-5.
31. Tanida I, Ueno T, Kominami E. LC3 conjugation system in *Mammalian* autophagy. Int J Biochem Cell Biol 2004;36:2503-18.
32. Duan P, Hu C, Quan C, Yu T, Zhou W, Yuan M, *et al.* 4-nonylphenol induces apoptosis, autophagy and necrosis in Sertoli cells: Involvement of ROS-mediated AMPK/AKT-mTOR and JNK pathways. Toxicology 2016;341-343:28-40.
33. Lu Y, Zhang R, Liu S, Zhao Y, Gao J, Zhu L, *et al.* ZT-25, a new vacuolar H(+)-ATPase inhibitor, induces apoptosis and protective autophagy through ROS generation in hepG2 cells. Eur J Pharmacol 2016;771:130-8.
34. Trachootham D, Alexandre J, Huang P. Targeting cancer cells by ROS-mediated mechanisms: A radical therapeutic approach? Nat Rev Drug Discov 2009;8:579-91.
35. Li L, Ishdorj G, Gibson SB. Reactive oxygen species regulation of autophagy in cancer: Implications for cancer treatment. Free Radic Biol Med 2012;53:1399-410.
36. Pelicano H, Carney D, Huang P. ROS stress in cancer cells and therapeutic implications. Drug Resist Updat 2004;7:97-110.
37. Simon HU, Haj-Yehia A, Levi-Schaffer F. Role of reactive oxygen species (ROS) in apoptosis induction. Apoptosis 2000;5:415-8.
38. Park KW, Kundu J, Chae IG, Kim DH, Yu MH, Kundu JK, *et al.* Carnosol induces apoptosis through generation of ROS and inactivation of STAT3 signaling in human colon cancer HCT116 cells. Int J Oncol 2014;44:1309-15.
39. Brunk UT, Dalen H, Roberg K, Hellquist HB. Photo-oxidative disruption of lysosomal membranes causes apoptosis of cultured human fibroblasts. Free Radic Biol Med 1997;23:616-26.
40. Chen Y, McMillan-Ward E, Kong J, Israels SJ, Gibson SB. Oxidative stress induces autophagic cell death independent of apoptosis in transformed and cancer cells. Cell Death Differ 2008;15:171-82.
41. Kiffin R, Bandyopadhyay U, Cuervo AM. Oxidative stress and autophagy. Antioxid Redox Signal 2006;8:152-62.
42. Chen L, Meng Y, Sun Q, Zhang Z, Guo X, Sheng X, *et al.* Ginsenoside compound K sensitizes human colon cancer cells to TRAIL-induced apoptosis via autophagy-dependent and – Independent DR5 upregulation. Cell Death Dis 2016;7:e2334.
43. Rauth S, Ray S, Bhattacharyya S, Mehrotra DG, Alam N, Mondal G, *et al.* Lupeol evokes anticancer effects in oral squamous cell carcinoma by inhibiting oncogenic EGFR pathway. Mol Cell Biochem 2016;417:97-110.
44. Liu Y, Bi T, Wang G, Dai W, Wu G, Qian L, *et al.* Lupeol inhibits proliferation and induces apoptosis of human pancreatic cancer PCNA-1 cells through AKT/ERK pathways. Naunyn Schmiedebergs Arch Pharmacol 2015;388:295-304.
45. Liu Y, Bi T, Shen G, Li Z, Wu G, Wang Z, *et al.* Lupeol induces apoptosis and inhibits invasion in gallbladder carcinoma GBC-SD cells by suppression of EGFR/MMP-9 signaling pathway. Cytotechnology 2016;68:123-33.
46. Saleem M, Murtaza I, Tarapore RS, Suh Y, Adhami VM, Johnson JJ, *et al.* Lupeol inhibits proliferation of human prostate cancer cells by targeting beta-catenin signaling. Carcinogenesis 2009;30:808-17.
47. Tarapore RS, Siddiqui IA, Adhami VM, Spiegelman VS, Mukhtar H. The dietary terpene lupeol targets colorectal cancer cells with constitutively active Wnt/β-catenin signaling. Mol Nutr Food Res 2013;57:1950-8.
48. Awad AB, Chinnam M, Fink CS, Bradford PG. Beta-sitosterol activates fas signaling in human breast cancer cells. Phytomedicine 2007;14:747-54.
49. Baskar AA, Ignacimuthu S, Paulraj GM, Al Numair KS. Chemopreventive potential of beta-sitosterol in experimental colon cancer model – An *in vitro* and *in vivo* study. BMC Complement Altern Med 2010;10:24.
50. von Holtz RL, Fink CS, Awad AB. Beta-sitosterol activates the sphingomyelin cycle and induces apoptosis in LNCaP human prostate cancer cells. Nutr Cancer 1998;32:8-12.